

# PCCP

Physical Chemistry Chemical Physics

Accepted Manuscript

This article can be cited before page numbers have been issued, to do this please use: Y. Jin, R. T. Saragi, M. Juanes, G. Feng and A. Lesarri, *Phys. Chem. Chem. Phys.*, 2021, DOI: 10.1039/D1CP00997D.



This is an Accepted Manuscript, which has been through the Royal Society of Chemistry peer review process and has been accepted for publication.

Accepted Manuscripts are published online shortly after acceptance, before technical editing, formatting and proof reading. Using this free service, authors can make their results available to the community, in citable form, before we publish the edited article. We will replace this Accepted Manuscript with the edited and formatted Advance Article as soon as it is available.

You can find more information about Accepted Manuscripts in the [Information for Authors](#).

Please note that technical editing may introduce minor changes to the text and/or graphics, which may alter content. The journal's standard [Terms & Conditions](#) and the [Ethical guidelines](#) still apply. In no event shall the Royal Society of Chemistry be held responsible for any errors or omissions in this Accepted Manuscript or any consequences arising from the use of any information it contains.

## ARTICLE

Interaction Topologies of the S...O Chalcogen Bond: The Conformational Equilibrium of the Cyclohexanol...SO<sub>2</sub> ClusterYan Jin,<sup>a,b</sup> Rizalina T. Saragi,<sup>b</sup> Marcos Juanes,<sup>b</sup> Gang Feng,<sup>\*a</sup> Alberto Lesarri<sup>\*b</sup>Received 00th January 20xx,  
Accepted 00th January 20xx

DOI: 10.1039/x0xx00000x

The conformational landscape of the cyclohexanol...SO<sub>2</sub> cluster was revealed in the gas phase using chirped-pulsed broadband rotational spectroscopy and quantum chemical calculations. Four isomers stabilized by a dominant S...O chalcogen bond and cooperative C-H...O=S and O-H...O=S secondary weak hydrogen bonds were observed, with a near-parallel orientation of the S=O and O-H bonds. Isomers formed by equatorial-*gauche* cyclohexanol are more stable than the isomers containing axial cyclohexanol. The multiple conformations of cyclohexanol and the versatile binding properties of SO<sub>2</sub>, simultaneously operating as nucleophile and electrophile through its  $\pi$ -holes and non-bonding electrons lead to a complex conformational behavior when the cluster is formed. The long (2.64 - 2.85 Å) attractive S...O interaction between SO<sub>2</sub> and cyclohexanol is mainly electrostatic and the contribution of charge transfer is obvious, with a NBO analysis suggesting that the strength of the S...O interaction is nearly two orders of magnitude larger than the hydrogen bonds. This study provides molecular insights into the structural and energetic characteristics that determine the formation of pre-nucleation clusters between SO<sub>2</sub> and a volatile organic compound like cyclohexanol.

## Introduction

Sulfur dioxide (SO<sub>2</sub>) is a major pollutant originated from coal burning and industrial emissions. Once in the atmosphere SO<sub>2</sub> operates as a source of sulfuric acid (H<sub>2</sub>SO<sub>4</sub>),<sup>1</sup> which serves as nucleating precursor for the formation of new larger atmospheric particles. Particle formation is explained by binary (H<sub>2</sub>SO<sub>4</sub>-H<sub>2</sub>O<sup>2</sup>), ternary (H<sub>2</sub>SO<sub>4</sub>-H<sub>2</sub>O-NH<sub>3</sub><sup>3</sup> and H<sub>2</sub>SO<sub>4</sub>-H<sub>2</sub>O-RNH<sub>2</sub><sup>4</sup>) or organic-enhanced<sup>5</sup> nucleation. Investigations also confirmed that SO<sub>2</sub> and SO<sub>3</sub> can form stable pre-nucleation clusters and therefore promote the formation of second organic aerosols (SOA).<sup>6</sup> Acquiring fundamental knowledge on the intermolecular interactions and binding topologies of sulfur nucleation centers is thus important for revealing initial processes in the formation of the critical nuclei. Field measurements and laboratory experiments on particle formation involving sulfur and organic compounds have mostly used aerosol chambers, mass spectrometry or photoelectron spectroscopy, but they do not provide a molecular description of the clusters.<sup>3,7</sup>

Among the gas-phase experiments, the combination of jet expansions and rotational spectroscopy<sup>8</sup> is a powerful tool for determining the preferred structures, binding topologies and molecular properties of intermolecular clusters, illustrating the structural and energetic features of the initial steps toward to the

formation of new atmospheric particles. Indeed, some rotational investigations of pre-nucleation clusters have been reported.<sup>9</sup> Interestingly, SO<sub>2</sub> may adopt multiple binding roles and exhibit a wide variety of binding interactions when forming intermolecular clusters. The nucleophilic n-pairs on the two terminal O atoms can form either hydrogen-bonds (HBs) to proton donors like HCl or HF,<sup>10</sup> or form halogen-bonds (XBs) to localized electron-deficient regions ( $\sigma$ -holes) within an halogen, as in SO<sub>2</sub>...ClF.<sup>11</sup> Alternatively, the charge holes<sup>12</sup> in the sulfur atom produce electrophilic regions acting as additional binding sites for S...O, S...N, S...S and S... $\pi$  chalcogen bonds (ChBs) with H<sub>2</sub>O,<sup>13</sup> CH<sub>3</sub>OH,<sup>14</sup> (CH<sub>3</sub>)<sub>2</sub>O,<sup>15</sup> HCN,<sup>16</sup> N(CH<sub>3</sub>)<sub>3</sub>,<sup>17</sup> H<sub>2</sub>S,<sup>18</sup> (CH<sub>3</sub>)<sub>2</sub>S<sup>19</sup> or the  $\pi$  electrons of C<sub>2</sub>H<sub>4</sub>,<sup>20</sup> C<sub>2</sub>H<sub>2</sub><sup>21</sup> and benzene.<sup>22</sup> ChBs are highly directional having strength comparable to HBs and sometimes even exceeding that of HBs,<sup>23</sup> conferring them a significant role in molecular recognition,<sup>24</sup> catalysis<sup>25</sup> and synthesis.<sup>26</sup> Cooperative or secondary weak HBs to the ChBs were also observed in several cases, further enhancing the stability of the clusters.<sup>14-15, 19</sup> However, only a single conformation has been observed for all the above SO<sub>2</sub> clusters. Conformational flexibility provides more possibilities for the formation and the subsequent growth of these clusters. The versatile conformations of SO<sub>2</sub> in forming clusters is still unclear, limiting the level of molecular understanding or how its intermolecular binding topology determines the conformational preference in multiconformational systems.

Herein cyclohexanol, a common volatile organic compound (VOC), is selected as the partner molecule to probe the multiple configurations of SO<sub>2</sub> in forming pre-nucleation clusters. Cyclohexanol has a certain degree of flexibility in its molecular structure. The ring inversion interconverts the alcohol group position, generating equatorial (*E*) and axial (*A*) conformers. In addition, the (low-barrier) internal rotation of the OH group generates *gauche* (*g*) and *anti* (*a*) orientations, and further

<sup>a</sup> School of chemistry and chemical engineering, Chongqing University, Daxuecheng South Rd. 55, Chongqing, 401331, China. E-mail: fengg@cqu.edu.cn

<sup>b</sup> Departamento de Química Física y Química Inorgánica — I.U. CINQUIMA, Universidad de Valladolid, Paseo de Belén, 7, 47011 Valladolid, Spain. E-mail: alberto.lesarri@uva.es

† Electronic Supplementary Information (ESI) available: molecular sketch of eight isomers (Figure S1); spectroscopic parameters of the eight isomers (Table S1); interconversion barrier connecting isomers I and II (Figure S2); experimental transition frequencies (Tables S2-S6); results of NBO analysis (Table S7) and results of the SAPT analysis of the eight isomers (Table S8). See DOI:

complicates the conformational potential energy surface, resulting in a total of four plausible cyclohexanol conformers, i.e. *Eg*, *Ea*, *Ag* and *Aa*. The two *gauche* orientations produce transient chirality, which is frozen on formation of clusters. Rotational spectroscopic investigations detected only the two equatorial conformers *Eg* and *Ea* in the gas phase, establishing that the *Eg* conformation is the global minimum followed by *Ea*.<sup>27</sup> The multiple conformations of cyclohexanol do not lead to a complex conformational behaviour when forming a cluster with water, since only one isomer, *Eg*-H<sub>2</sub>O, has been observed.<sup>27</sup> However, multiple conformations showed up for the cyclohexanol dimer, in which six isomers have been identified.<sup>28</sup>

In this study, the multiple conformations and binding features of the cyclohexanol...SO<sub>2</sub> cluster were investigated by using chirped-pulsed Fourier transform microwave (CP-FTMW) spectroscopy and quantum chemical calculations.

## Methods

### Rotational spectroscopy

The rotational spectrum was measured with a broadband pulsed-jet direct-digital chirped-pulsed Fourier transform microwave (FTMW) spectrometer at the University of Valladolid,<sup>29</sup> working in the frequency range of 2-8 GHz. In this spectrometer, a (4 μs) chirp pulse is created by an arbitrary waveform generator, amplified to 20 W and radiated into the jet. The molecular transient emission created from rotational decoherence extends for ca. 40 μs per excitation pulse and is recorded by using a (250 MS/s) digital oscilloscope. Commercial samples of cyclohexanol and SO<sub>2</sub> were used without further treatment. Cyclohexanol was put inside a reservoir nozzle and vaporized *in situ* at 50°C. The molecular cluster was then generated by co-expanding cyclohexanol with a stream of a gaseous mixture of SO<sub>2</sub> (0.5%) diluted in neon at backing pressures of 0.2 MPa. The final spectrum was obtained by averaging 1 M free-induction-decays in the time-domain and was Fourier transformed to provide the frequency-domain spectrum. The spectral linewidths after the Fourier transformation (Kaiser-Bessel window) are ca. 150 kHz (FWHM). The accuracy of the frequency measurements is estimated to be better than 10 kHz.

### Computational methods

The possible conformations of the cyclohexanol-SO<sub>2</sub> cluster were first explored with a conformational search based on molecular mechanics and the MMFFs force field<sup>30</sup> (implemented in MacroModel<sup>31</sup>). The initial structures were subject to full geometry optimizations and harmonic vibrational frequency calculations using the B3LYP<sup>32</sup> method including two-body Grimme's D3<sup>33</sup> dispersion corrections with Becke-Johnson (BJ) damping,<sup>34</sup> employing the def2-TZVP and the aug-cc-pVTZ basis sets. The basis-set superposition error (BSSE)<sup>35</sup> was corrected with the counterpoise (CP) method. A Natural Bond Orbital (NBO) analysis<sup>36</sup> was performed at the B3LYP-D3(BJ)/aug-cc-pVTZ level. All the calculations were implemented in the Gaussian16 program package.<sup>37</sup>

The Multiwfn program<sup>38</sup> and VMD software<sup>39</sup> were used to perform the non-covalent interaction (NCI)<sup>40</sup> analysis. Finally, a Symmetry-Adapted Perturbation Theory (SAPT)<sup>41</sup> analysis was

implemented at the SAPT2+(3)δMP2/aug-cc-pVDZ level by using the PSI4 program<sup>42</sup> to produce an energy decomposition.

## Results and discussion

### Theoretical Results

Eight isomers with relative energies within 500 cm<sup>-1</sup> were initially predicted for the cyclohexanol...SO<sub>2</sub> cluster (Figure S1 and Table S1, ESI<sup>†</sup>) using the B3LYP-D3(BJ)/def2-TZVP method. The first five most stable isomers displayed in Figure 1 were later reoptimized at the B3LYP-D3(BJ)/aug-cc-pVTZ level. The global minimum (isomer *Eg*\_SO<sub>2</sub>\_1) is constituted by *Eg* cyclohexanol, with all atoms of SO<sub>2</sub> simultaneously interacting with the alcohol and the ring hydrogens. The *Eg* cyclohexanol is also the conformation found in isomer *Eg*\_SO<sub>2</sub>\_2, while isomer *Ea*\_SO<sub>2</sub>\_1 contains *Ea* cyclohexanol. The cyclohexanol moiety in isomers *Ag*\_SO<sub>2</sub>\_1 and *Aa*\_SO<sub>2</sub>\_1 adopts the *Ag* and *Aa* conformations, respectively. Table 1 reports the calculated rotational constants, electric dipole moment components and relative energies of the five most stable isomers. The zero-point and counterpoise corrected interaction energies of the five isomers are also given in Table 1.

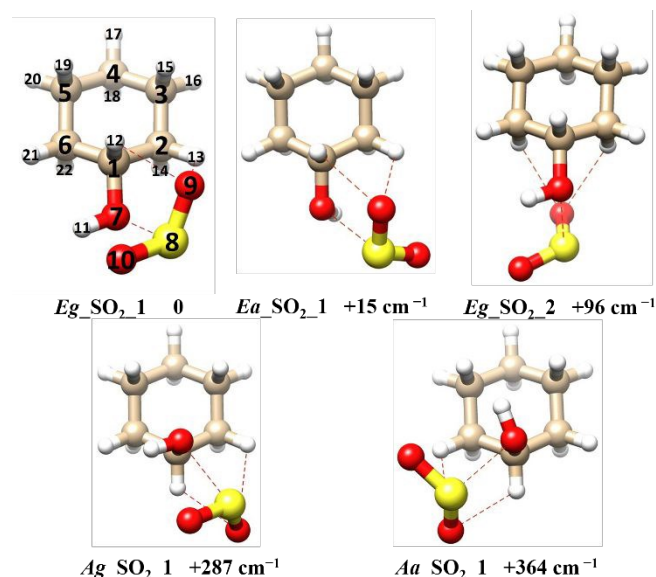


**Figure 1.** B3LYP-D3(BJ)/aug-cc-pVTZ calculated molecular structures, relative electronic energies (zero-point and counterpoise corrected) and atom numbering of the five lowest-lying isomers of the cyclohexanol...SO<sub>2</sub> cluster.

**Table 1.** Rotational parameters of the first five stable isomers of cyclohexanol...SO<sub>2</sub> calculated at the B3LYP-D3(BJ)/aug-cc-pVTZ level of theory.<sup>a</sup>

	<i>Eg</i> _SO <sub>2</sub> _1	<i>Ea</i> _SO <sub>2</sub> _1	<i>Eg</i> _SO <sub>2</sub> _2	<i>Ag</i> _SO <sub>2</sub> _1	<i>Aa</i> _SO <sub>2</sub> _1
<i>A<sub>e</sub></i> /MHz	2479.05	2408.89	2124.13	2517.30	2363.22
<i>B<sub>e</sub></i> /MHz	527.00	535.48	568.16	538.64	575.52
<i>C<sub>e</sub></i> /MHz	479.39	502.14	561.96	500.22	536.64
<i>μ<sub>a</sub></i>  /D	2.54	2.40	2.22	2.70	2.75
<i>μ<sub>b</sub></i>  /D	0.47	1.16	0.74	0.12	0.47
<i>μ<sub>c</sub></i>  /D	0.87	0.74	1.08	0.42	0.75
Δ <i>E<sub>0</sub></i> /cm <sup>-1</sup>	0	13	94	288	361
Δ <i>G</i> /kJ mol <sup>-1</sup>	0.0	0.0	1.1	0.4	0.1
<i>D<sub>0,BSSE</sub></i> /kJ mol <sup>-1</sup>	-28.2	-28.3	-27.0	-27.8	-28.7

<sup>a</sup> Equilibrium rotational constants (*A<sub>e</sub>*, *B<sub>e</sub>*, *C<sub>e</sub>*), dipole moment components in the principal inertial axes system (*μ<sub>α</sub>*, α = a, b, c), electronic (Δ*E<sub>0</sub>*), Gibbs (Δ*G*) and complexation energies (*D<sub>0,BSSE</sub>*).

### Rotational spectra

Using the theoretical predictions in Table 1, four different sets of rotational spectra were positively assigned to isomers **Eg\_SO<sub>2</sub>\_1**, **Eg\_SO<sub>2</sub>\_2**, **Ag\_SO<sub>2</sub>\_1** and **Aa\_SO<sub>2</sub>\_1**. A section of the spectrum is given in Figure 2, showing the *R*-branch ( $J + 1 \leftarrow J = 5 \leftarrow 4$  *a*-type transitions with  $K_a = 0, 1, 2$  of the four detected isomers together with other transitions of isomers **Eg\_SO<sub>2</sub>\_1** and **Eg\_SO<sub>2</sub>\_2**. For isomer **Eg\_SO<sub>2</sub>\_1**, the rotational spectrum of the mono-substituted <sup>34</sup>S species was also measured in natural abundance (~4%). None of the observed transitions showed tunnelling splittings associated to the internal motion of the SO<sub>2</sub> moiety or the torsion of the OH group of cyclohexanol, suggesting that the two subunits are rigidly linked or that complexation quenches plausible tunnelling motions in the dimer.

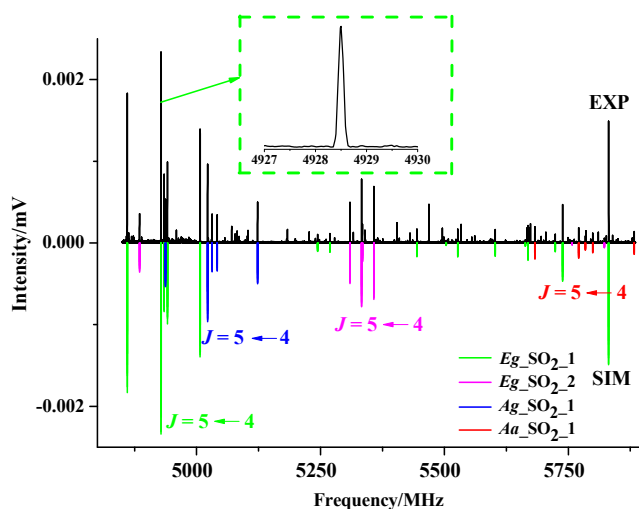


**Figure 2.** A section of the measured rotational spectrum in the 4850-5885 MHz range, showing the assignment of four isomers of cyclohexanol...SO<sub>2</sub>. The positive trace shows the experimental transitions belonging to isomers **Eg\_SO<sub>2</sub>\_1**, **Eg\_SO<sub>2</sub>\_2**, **Ag\_SO<sub>2</sub>\_1** and **Aa\_SO<sub>2</sub>\_1**. The negative trace represents the fit results of Table 2, with different colours for each isomer. The inset shows a typical rotational transition ( $5_{04} \leftarrow 4_{04}$ ) of isomer **Eg\_SO<sub>2</sub>\_1**. The spectrum was simulated at a rotational temperature of 1 K and used the theoretical values of the dipole moments reported in Table 1.

The rotational transitions were fitted independently to the Watson's *S*-reduction semi-rigid rotor Hamiltonian (*I'* representation),<sup>43</sup> implemented in Pickett's SPCAT/SPFIT programs.<sup>44</sup> The determined spectroscopic parameters of the four isomers and the <sup>34</sup>S isotopologue of isomer **Eg\_SO<sub>2</sub>\_1** are reported

in Table 2. The details of the spectral measurements and analysis along with all the assigned transitions are given in the Supporting Information (Tables S2-S6, ESI<sup>†</sup>).

The isomer identification confirmed that both equatorial (*Eg*) and axial (*Ag* and *Aa*) conformers of cyclohexanol are present in the clusters with SO<sub>2</sub>. The global minimum (isomer **Eg\_SO<sub>2</sub>\_1**) is formed by the most stable conformer of cyclohexanol (*Eg*), with the versatile SO<sub>2</sub> engaging in a dominant S...O chalcogen bond and apparently additional secondary C-H...O=S and O-H...O=S hydrogen bonds as attractive forces for stabilizing the cluster. All other isomers share the S...O bond, but present different SO<sub>2</sub> contacts to the ring. The second detected isomer (**Eg\_SO<sub>2</sub>\_2**) also contains *Eg* cyclohexanol, but SO<sub>2</sub> approaches the opposite side of the ring, linking to a different lone pair of the cyclohexanol oxygen. The isomers with lower populations formed by the *Ag* and *Aa* forms (**Ag\_SO<sub>2</sub>\_1** and **Aa\_SO<sub>2</sub>\_1**) combine also multiple interactions primarily governed by a S...O bond.

### Conformations and molecular structure

The relative abundance of the four isomers in the supersonic jet was estimated by their spectral intensities and the electric dipole moment components in Table 1, assuming a linear fast-passage excitation regime (intensities proportional to the square dipole moments) and uniform instrumental response.<sup>45</sup> This estimation gives a population ratio of  $N(\mathbf{Eg\_SO_2\_1}) : N(\mathbf{Eg\_SO_2\_2}) : N(\mathbf{Ag\_SO_2\_1}) : N(\mathbf{Aa\_SO_2\_1}) = 16.7 : 7.6 : 4.5 : 1$ , in qualitative agreement with the calculated conformational ordering of 5.8 : 5.4 : 3.7 : 1. The discrepancy is attributed to kinetic effects in the jet, including collisional population transfer<sup>46</sup> and enhanced preference for the most abundant monomer conformations.<sup>47</sup> No isomer containing *Ea* cyclohexanol could be found, especially that of isomer **Ea\_SO<sub>2</sub>\_1**, which is predicted to be the second most stable structure. A calculation of the conformational interconversion from isomer **Ea\_SO<sub>2</sub>\_1** to **Eg\_SO<sub>2</sub>\_1** gives a potential energy barrier of ~298 cm<sup>-1</sup> (Figure S2), indicating that conformational relaxation<sup>46</sup> likely occurs in the supersonic jet which therefore prevents the detection of isomer **Ea\_SO<sub>2</sub>\_1**. A calculated conformational ordering of 11.5 : 5.4 : 3.7 : 1 is obtained considering the population transfer of **Ea\_SO<sub>2</sub>\_1** to **Eg\_SO<sub>2</sub>\_1**, closer to the experimental estimation. For the only isomer with all selection rules active, **Ag\_SO<sub>2</sub>\_1**, the experimental ratios  $\mu_a : \mu_b : \mu_c$  are estimated as 18:1:2.7, in qualitative agreement with the predicted values of the dipole moment components.

**Table 2.** Experimental rotational parameters of the dimer cyclohexanol...SO<sub>2</sub>.

	<b>Eg_SO<sub>2</sub>_1</b>	<b>Eg_SO<sub>2</sub>_1-<sup>34</sup>S</b>	<b>Eg_SO<sub>2</sub>_2</b>	<b>Ag_SO<sub>2</sub>_1</b>	<b>Aa_SO<sub>2</sub>_1</b>
$A_0$ /MHz <sup>a</sup>	2430.1591(9) <sup>d</sup>	2428.2(6)	2137.020(3)	2506.4(2)	2187.2(3)
$B_0$ /MHz	508.2381(3)	500.7532(7)	538.1844(6)	521.8200(4)	598.6738(6)
$C_0$ /MHz	478.8195(3)	472.1942(6)	528.5905(6)	484.6814(4)	558.5563(6)
$D_J$ /kHz	0.196(3)	0.196(3) <sup>e</sup>	0.252(7)	0.094(3)	0.465(6)
$D_{JK}$ /kHz	-0.81(2)	-0.81(2) <sup>e</sup>	-1.04(5)	0.49(3)	2.8(1)
$ \mu_a $ <sup>b</sup>	+++	+++	+++	+++	+++
$ \mu_b $	++	None	+	None	None
$ \mu_c $	None	None	++	None	None
$N$ <sup>c</sup>	63	17	40	32	22
$\sigma$ /kHz	7.1	8.9	9.9	4.9	5.2

<sup>a</sup> Ground-state rotational constants ( $A_0$ ,  $B_0$ ,  $C_0$ ) and Watson's *S*-reduction centrifugal distortion constants ( $D_J$  and  $D_{JK}$ ;  $D_{K_2}$ ,  $d_1$  and  $d_2$  were fixed to zero). <sup>b</sup> A positive sign indicates the observation of the corresponding type of transitions. <sup>c</sup> Number of transitions in the fit ( $N$ ) and root-mean-square (RMS) error ( $\sigma$ ). <sup>d</sup> Errors in parenthesis are  $1\sigma$  uncertainties expressed in units of the last digit.

**Table 3.** Experimental structural parameters ( $r_0$ ) compared with the theoretical ( $r_e$ ) values (distances in Å, angles in degrees).

<i>Eg_SO2_1</i>	$r_{0758}$	$r_{010H11}$	$r_{09H12}$	$r_{09H13}$	$\angle S8O7C1$	$\angle S8O7C1C6$	$\angle H11O7C1C4$	$\angle O10S8O7H11$
$r_e^a$	2.578	2.755	2.609	2.926	109.9	86.0	-112.5	-2.7
$r_0$	2.638(5) <sup>b</sup>	-	-	-	108.4(2)	105.6(3)	-	-
<i>Eg_SO2_2</i>	$r_{0758}$	$r_{010H11}$	$r_{09H14}$	$r_{09H22}$	$\angle S8O7C6$	$\angle S8O7C1C6$	$\angle H11O7C1C4/$	$\angle O10S8O7H11$
$r_e$	2.620	2.790	2.740	2.685	101.4	57.2	-117.9	4.0
$r_0$	2.70(2)	-	-	-	105.8(6)	-	-	-
<i>Ag_SO2_1</i>	$r_{0758}$	$r_{010H11}$	$r_{09H12}$	$r_{09H13}$	$\angle S8O7C1$	$\angle S8O7C1C2$	$\angle H11O7C1C4$	$\angle O10S8O7H11$
$r_e$	2.572	2.738	2.624	2.988	109.6	-86.2	109.5	2.2
$r_0$	2.6894(8)	-	-	-	-	-83.0(1)	-	-
<i>Aa_SO2_1</i>	$r_{0758}$	$r_{010H11}$	$r_{09H12}$	$r_{09H21}$	$\angle S8O7C1$	$\angle S8O7C2C3$	$\angle H11O7C1C4$	$\angle O10S8O7H11$
$r_e$	2.567	2.991	2.664	2.910	111.1	145.1	19.0	17.5
$r_0$	2.848(5)	-	-	-	-	101.4(6)	-	-

<sup>a</sup> The  $r_e$  structure was calculated at B3LYP-D3(BJ)/aug-cc-pVTZ levels of theory. <sup>b</sup> Errors in parenthesis are 1 $\sigma$  uncertainties expressed in units of the last digit.

The experimental rotational constants reported in Table 2 were used to determine effective ( $r_0$ ) structures of the observed isomers through a least-squares fit procedure,<sup>48</sup> assuming that the ring skeleton and SO<sub>2</sub> are not perturbed upon complexation. Since only limited isotopic data were available (two sets of rotational constants for the most stable isomer and one set of rotational constants for other three observed isomer), only the structural parameters involving the intermolecular internal coordinates were adjusted to fit the rotational constants to the experimental ones, while keeping the structural parameters of the isomers fixed at the B3LYP-D3(BJ)/aug-cc-pVTZ predicted values. The derived structural parameters concerning the non-covalent interactions for the four observed isomers of cyclohexanol...SO<sub>2</sub> are reported in Table 3 (the equilibrium structures or  $r_e$  are also present for comparison). The S...O distances are in the range of 2.64 - 2.85 Å with the shortest distance observed in isomer *Eg\_SO2\_1* (2.638(5) Å). These distances are significantly shorter than that of S...O ChB determined for the 2,2,4,4-tetrafluoro-1,3-dithietane (C<sub>2</sub>S<sub>2</sub>F<sub>4</sub>)...water cluster (2.912(5) Å).<sup>49</sup> The distances of C-H...O=S and O-H...O=S in the four isomers are in the range of 2.6 - 3.0 Å and 2.7 - 3.0 Å, respectively, structurally suggesting the existence of these secondary interactions. The presence of secondary interactions determining the conformational preference was also revealed in the chalcogen bonded clusters of C<sub>2</sub>S<sub>2</sub>F<sub>4</sub>.<sup>49,50</sup> The dihedral angles H11O7C1C4 (Table 3) are slightly changed in the cluster compared to that of the cyclohexanol monomer (-120.3° for *Eg*, 116.4° for *Ag*, 0.0° for *Aa*) to better accommodate the intermolecular interactions.

### Non-covalent interactions

The non-covalent interactions between cyclohexanol and SO<sub>2</sub> are visualized through NCI plots in Figure 3, using a reduced gradient of the electronic density.<sup>51</sup> The results show that the dominant S...O ChB interaction contribute to the stabilization of all isomers. The C-H...O=S interaction cooperatively stabilizes the observed isomers while O-H...O=S interaction is rather weak and is not present in the NCI plots. Figure 4 reports the plot of the electronic reduced density gradient (RDG) versus the signed density (sign( $\lambda_2$ ) $\rho$ ) for the four observed isomers, further indicating the existence of S...O ChB and weak attractive intermolecular interactions.

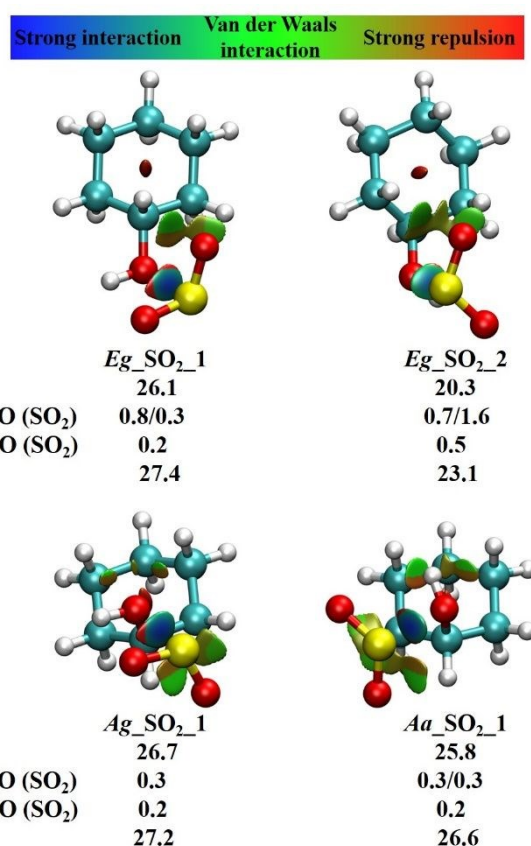


**Figure 3.** The NCI plots and the NBO analysis showing stabilization energy contributions ( $\geq 0.2$  kJ mol<sup>-1</sup>) for the four isomers of the cyclohexanol...SO<sub>2</sub> cluster.

The strength of each kind of NCI was quantitatively evaluated by a NBO analysis. The results of the NBO analysis are given in Figure 3 and Table S7 (ESI<sup>†</sup>). The second-order perturbation stabilization energies ( $E^{(2)}$ ) for the S...O ChB in the four isomers are calculated to be 23.1 - 27.4 kJ mol<sup>-1</sup>, representing the largest contribution to the stabilization of the clusters. The C-H...O=S and O-H...O=S interactions have very weak interaction energies (larger for C-H...O=S) in the range of 0.2 - 1.6 kJ mol<sup>-1</sup>, but are clearly identified

as necessary contributors to the cluster stabilization. Isomer **Eg\_SO<sub>2</sub>\_1** has the highest total interaction energy (27.4 kJ mol<sup>-1</sup>), followed by isomers **Ag\_SO<sub>2</sub>\_1** and **Aa\_SO<sub>2</sub>\_1**. The NBO analysis thus supports the experimentally observed structural preferences of the cluster, which simultaneously depend both on the cyclohexanol conformational equilibria and the peculiar strength of NCIs formed between the subunits, in particular the chalcogen bond. The total interaction energies from the NBO analysis are consistent with the zero-point and counterpoise-corrected interaction energies calculated at the B3LYP-D3(BJ)/aug-cc-pVTZ level of theory (Table 1).

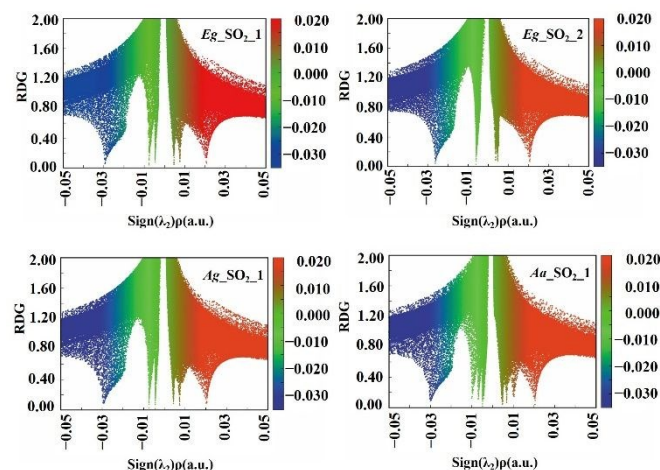


**Figure 4.** The scatter diagram of the electronic density reduced density gradient (RDG) vs the signed density ( $\text{sign}(\lambda_2)\rho$ ) for the four isomers of the cyclohexanol...SO<sub>2</sub> cluster.

**Table 4.** The SAPT energy decomposition analysis for the four isomers of the cyclohexanol...SO<sub>2</sub> cluster, the most stable isomer of cyclohexanol dimer, cyclohexanol-H<sub>2</sub>O, SO<sub>2</sub>-H<sub>2</sub>O and water dimer (all energy values in kJ mol<sup>-1</sup>).

	$E_{\text{elec.}}$	$E_{\text{dis.}}$	$E_{\text{ind.}}$	$E_{\text{exc.}}$	CT	Total
<b>Eg_SO<sub>2</sub>_1</b>	-68.5	-25.8	-31.6	82.8	-17.6	-43.1
<b>Eg_SO<sub>2</sub>_2</b>	-64.2	-25.6	-27.8	74.6	-14.6	-43.0
<b>Ag_SO<sub>2</sub>_1</b>	-68.5	-25.6	-31.6	83.2	-17.8	-42.5
<b>Aa_SO<sub>2</sub>_1</b>	-70.4	-26.8	-32.2	84.4	-17.9	-45.0
(Cyclohexanol) <sub>2</sub>	-47.0	-30.2	-17.2	63.4	-5.7	-30.9
Cyclohexanol...H <sub>2</sub> O	-46.1	-15.6	-14.8	53.1	-5.8	-23.5
SO <sub>2</sub> ...H <sub>2</sub> O	-46.3	-12.5	-16.6	58.9	-10.5	-16.6
(H <sub>2</sub> O) <sub>2</sub>	-36.3	-7.6	-9.2	36.2	-4.9	-16.9

The physical nature of the NCIs contributing to the stability of the four detected isomers is revealed by energy decomposition with a SAPT analysis. This approach provides an estimation of the contribution of electrostatic ( $E_{\text{elec.}}$ ), dispersion ( $E_{\text{dis.}}$ ), induction ( $E_{\text{ind.}}$ ) and exchange-repulsion ( $E_{\text{exc.}}$ ) to the total interaction energy and the contribution of charge transfer (CT). The results of the SAPT analysis for the four observed isomers are reported in Table 4. The SAPT total interaction energies are in the range of -42.5 to -45.0 kJ mol<sup>-1</sup>. The main term of the attractive energy of the cyclohexanol...SO<sub>2</sub> cluster is electrostatic, accounting for 54.4%, 54.9%, 54.5% and 54.4% of the attractive interactions for isomers **Eg\_SO<sub>2</sub>\_1**, **Eg\_SO<sub>2</sub>\_2**, **Ag\_SO<sub>2</sub>\_1** and **Aa\_SO<sub>2</sub>\_1**, respectively. The induction and dispersion energy terms are comparable in magnitude. The contribution of charge transfer to the interaction energy is obvious, accounting for 14.0%, 12.4%, 14.2% and 13.8% of the total attractive energy for isomers **Eg\_SO<sub>2</sub>\_1**, **Eg\_SO<sub>2</sub>\_2**, **Ag\_SO<sub>2</sub>\_1** and **Aa\_SO<sub>2</sub>\_1**, respectively. This charge transfer feature is consistent with the observations in the SO<sub>2</sub>...dimethyl sulfide (DMS) cluster, where remarkable charge

transfer between the sulfur atoms of DMS and SO<sub>2</sub> has been observed.<sup>19</sup> The total SAPT interaction energies of cyclohexanol...SO<sub>2</sub> (-43 to -45 kJ mol<sup>-1</sup>) are larger than the calculations in Table 1 and also about 12 and 27 kJ mol<sup>-1</sup> larger than the C<sub>2</sub>S<sub>2</sub>F<sub>4</sub>...isopropylamine<sup>50b</sup> and C<sub>2</sub>S<sub>2</sub>F<sub>4</sub>...water<sup>49</sup> clusters, respectively.

The SAPT analyses for the cyclohexanol dimer, H<sub>2</sub>O dimer, cyclohexanol...H<sub>2</sub>O and SO<sub>2</sub>...H<sub>2</sub>O were also carried out for comparison (Table 4). The total interaction energy of cyclohexanol...SO<sub>2</sub> ranks the highest among these clusters. Especially, the total interaction energy of cyclohexanol...SO<sub>2</sub> is about 2.5 times of that of SO<sub>2</sub>...H<sub>2</sub>O, in which a S...O ChB is the main contribution of the stabilization. These results suggest that the formation of cyclohexanol...SO<sub>2</sub> cluster (or more general alcohol...SO<sub>2</sub> cluster) is likely preferred in the atmosphere when alcohol precursors, SO<sub>2</sub> and water are co-present.

## Conclusions

In conclusion, the binary intermolecular cluster formed by cyclohexanol and SO<sub>2</sub> was investigated in the gas phase by chirped-pulsed microwave spectroscopy and quantum chemical computations. Four isomers, in which the cyclohexanol moiety adopts *Eg*, *Ag* and *Aa* conformations, were observed in the jet expansion. The S...O ChB is the dominant attractive force in forming the cluster. Secondary and relatively weaker C-H...O=S hydrogen bonds contribute further stabilization to the cluster, with SAPT calculations suggesting that electrostatics is the main contributor to the attractive energy. No isomer containing *Ea* cyclohexanol could be observed. Since binding energies are relatively similar for all isomers (differing less than 1.7 kJ mol<sup>-1</sup> in Table 1), the experimental jet-cooled conformational preferences of the cyclohexanol...SO<sub>2</sub> cluster are affected by collisional relaxation<sup>46</sup> and by the population<sup>47</sup> and conformational preferences of the cyclohexanol monomer (*Ag* and *Aa* are calculated to be ~1.8 kJ mol<sup>-1</sup> and 5.7 kJ mol<sup>-1</sup> higher in energy than that of *Eg*<sup>27</sup>). The multiple conformations of cyclohexanol and the versatile binding properties of SO<sub>2</sub> thus lead to a complex conformational behaviour when the cluster is formed. The present work adds accurate information on the evasive S...O chalcogen bond, mostly studied in condensed phases or by theoretical methods, emphasizing the factual value of gas-phase investigations for the analysis of weakly-bound molecular clusters in isolation conditions.

## Conflicts of interest

There are no conflicts to declare.

## Acknowledgements

We thank Chongqing University and the Spanish MICINN-FEDER (PGC2018-098561-B-C22) for financial support. Y. Jin thanks the China Scholarships Council (CSC) for a scholarship (201906050058).

## Author Contributions

Yan Jin, Rizalina T. Saragi performed the experiment;

Yan Jin, Rizalina T. Saragi, Marcos Juanes contributed to the theoretical calculation and analysis;

Yan Jin, Gang Feng, Alberto Lesarri performed the data analyses and wrote the manuscript;

Gang Feng, Alberto Lesarri contributed to the conception and supervision of the study.

## Notes and references

- J. G. Calvert, A. Lazrus, G. L. Kok, B. G. Heikes, J. G. Walega, J. Lind, C. A. Cantrell, *Nature* 1985, **317**, 27.
- M. Sipilä, T. Berndt, T. Petäjä, D. Brus, J. Vanhanen, F. Stratmann, J. Patokoski, R. L. M. III, A.-P. Hyvärinen, H. Lihavainen, M. Kulmala, *Science* 2010, **327**, 1243.
- D. J. Coffman, D. A. Hegg, *J. Geophys. Res.* 1995, **100**, 7147.
- a)M. E. Erupe, A. A. Viggiano, S.-H. Lee, *Atmos. Chem. Phys.* 2011, **11**, 4767; b)J. Almeida, S. Schobesberger, A. Kurten, I. K. Ortega, O. Kupiainen-Maatta, A. P. Praplan, A. Adamov, A. Amorim, F. Bianchi, M. Breitenlechner, A. David, J. Dommen, N. M. Donahue, A. Downard, E. Dunne, J. Duplissy, S. Ehrhart, R. C. Flagan, A. Franchin, R. Guida, J. Hakala, A. Hansel, M. Heinritzi, H. Henschel, T. Jokinen, H. Junninen, M. Kajos, J. Kangasluoma, H. Keskinen, A. Kupc, T. Kurten, A. N. Kvashin, A. Laaksonen, K. Lehtipalo, M. Leiminger, J. Leppa, V. Loukonen, V. Makhmutov, S. Mathot, M. J. McGrath, T. Nieminen, T. Olenius, A. Onnela, T. Petaja, F. Riccobono, I. Riipinen, M. Rissanen, L. Rondo, T. Ruuskanen, F. D. Santos, N. Sarnela, S. Schallhart, R. Schnitzhofer, J. H. Seinfeld, M. Simon, M. Sipila, Y. Stozhkov, F. Stratmann, A. Tome, J. Trostl, G. Tsagkogeorgas, P. Vaattovaara, Y. Viisanen, A. Virtanen, A. Vrtala, P. E. Wagner, E. Weingartner, H. Wex, C. Williamson, D. Wimmer, P. Ye, T. Yli-Juuti, K. S. Carslaw, M. Kulmala, J. Curtius, U. Baltensperger, D. R. Worsnop, H. Vehkamäki, J. Kirkby, *Nature* 2013, **502**, 359.
- a)R. Zhang, I. Suh, J. Zhao, D. Zhang, E. C. Fortner, X. Tie, L. T. Molina, M. J. Molina, *Science* 2004, **304**, 1487; b)S. Schobesberger, H. Junninen, F. Bianchi, G. Lonn, M. Ehn, K. Lehtipalo, J. Dommen, S. Ehrhart, I. K. Ortega, A. Franchin, T. Nieminen, F. Riccobono, M. Hutterli, J. Duplissy, J. Almeida, A. Amorim, M. Breitenlechner, A. J. Downard, E. M. Dunne, R. C. Flagan, M. Kajos, H. Keskinen, J. Kirkby, A. Kupc, A. Kurten, T. Kurten, A. Laaksonen, S. Mathot, A. Onnela, A. P. Praplan, L. Rondo, F. D. Santos, S. Schallhart, R. Schnitzhofer, M. Sipilä, A. Tome, G. Tsagkogeorgas, H. Vehkamäki, D. Wimmer, U. Baltensperger, K. S. Carslaw, J. Curtius, A. Hansel, T. Petaja, M. Kulmala, N. M. Donahue, D. R. Worsnop, *Proc. Natl. Acad. Sci. U.S.A.* 2013, **110**, 17223.
- a)L. Xu, H. Guo, C. M. Boyd, M. Klein, A. Bougiatioti, K. M. Cerully, J. R. Hite, G. Isaacman-VanWertz, N. M. Kreisberg, C. Knote, K. Olson, A. Koss, A. H. Goldstein, S. V. Hering, J. d. Gouw, K. Baumann, S.-H. Lee, A. Nenes, R. J. Weber, N. L. Ng, *Proc. Natl. Acad. Sci. U.S.A.* 2015, **112**, E4506; b)J. Ye, J. P. D. Abbatt, A. W. H. Chan, *Atmos. Chem. Phys.* 2018, **18**, 5549; c)S. Liu, L. Jia, Y. Xu, N. T. Tsona, S. Ge, L. Du, *Atmos. Chem. Phys.* 2017, **17**, 13329; d)Z. Yang, N. T. Tsona, J. Li, S. Wang, L. Xu, B. You, L. Du, *Environ. Pollut.* 2020, **264**, 114742; e)P. M. Pawlowski, S. R. Okimoto, F.-M. Tao, *J. Phys. Chem. A* 2003, **107**, 5327; f)S. W. Hunt, C. S. Brauer, M. B. Craddock, K. J. Higgins, A. M. Nienow, K. R. Leopold, *Chem. Phys.* 2004, **305**, 155. DOI: 10.1039/D1CP00997D
- a)R. Zhang, L. Wang, A. F. Khalizov, J. Zhao, J. Zheng, R. L. McGraw, L. T. Molina, *Proc. Natl. Acad. Sci. U.S.A.* 2009, **106**, 17650; b)G. L. Hou, W. Lin, S. H. Deng, J. Zhang, W. J. Zheng, F. Paesani, X. B. Wang, *J. Phys. Chem. Lett.* 2013, **4**, 779; c)G. L. Hou, X. B. Wang, *Acc. Chem. Res.* 2020, **53**, 2816.
- a)M. Juanes, R. T. Saragi, W. Caminati, A. Lesarri, *Chem. Eur. J.* 2019, **25**, 11402; b)W. Caminati, J.-U. Grabow, in *Frontiers and Advances in Molecular Spectroscopy* Elsevier, Amsterdam, 2018.
- a)M. K. Jahn, E. Mendez, K. P. R. Nair, P. D. Godfrey, D. McNaughton, P. Eciija, F. J. Basterretxea, E. J. Cocinero and J.-U. Grabow, *Phys. Chem. Chem. Phys.* 2015, **17**, 19726; b)A. Vigorito, Q. Gou, C. Calabrese, S. Melandri, A. Maris and W. Caminati, *ChemPhysChem* 2015, **16**, 2961-2967.
- A. J. Fillery-Travis, A. C. Legon, *Chem. Phys. Lett.* 1986, **123**, 4.
- G. Cotti, J. H. Holloway, A. C. Legon, *Chem. Phys. Lett.* 1996, **255**, 401.
- a)A. Bauzá, T. J. Mooibroek, A. Frontera, *ChemPhysChem.* 2015, **16**, 2496.
- K. Matsumura, F. J. Lovas, R. D. Suenram, *J. Chem. Phys.* 1989, **91**, 5887.
- L. Sun, X. Q. Tan, J. J. Oh, R. L. Kuczkowski, *J. Chem. Phys.* 1995, **103**, 6440.
- J. J. Oh, K. W. Hillig, R. L. Kuczkowski, *Inorg. Chem.* 1991, **30**, 4583.
- E. J. Goodwin, A. C. Legon, *J. Chem. Phys.* 1986, **85**, 6828.
- J. J. Oh, M. S. LaBarge, J. Matos, J. W. Kampf, K. W. Hillig, R. L. Kuczkowski, *J. Am. Chem. Soc.* 1991, **113**, 4732.
- R. E. Bumgarner, D. J. Pauley, S. G. Kukolich, *J. Chem. Phys.* 1987, **87**, 3749.
- D. A. Obenchain, L. Spada, S. Alessandrini, S. Rampino, S. Herbers, N. Tasinato, M. Mendolicchio, P. Kraus, J. Gauss, C. Puzzarini, J.-U. Grabow, V. Barone, *Angew. Chem. Int. Ed.* 2018, **57**, 15822.
- A. M. Andrews, A. Taleb-Bendiab, M. S. LaBarge, K. W. Hillig, R. L. Kuczkowski, *J. Chem. Phys.* 1990, **93**, 7030.
- A. M. Andrews, K. W. Hillig, R. L. Kuczkowski, A. C. Legon, N. W. Howard, *J. Chem. Phys.* 1991, **94**, 6947.
- A. Taleb-Bendiab, K. W. Hillig, R. L. Kuczkowski, *J. Chem. Phys.* 1992, **97**, 2996.
- a)A. C. Legon, *Phys. Chem. Chem. Phys.* 2017, **19**, 14884; b) P. Scilabra, G. Terraneo, G. Resnati, *Acc. Chem. Res.*, 2019, **52**, 1313; c)V. P. N. Nziko, S. Scheiner, *J. Phys. Chem. A* 2014, **118**, 10849.
- N. Biot, D. Bonifazi, *Coord. Chem. Rev.* 2020, **413**, 213243.
- S. Benz, A. I. Poblador-Bahamonde, N. Low-Ders, S. Matile, *Angew. Chem. Int. Ed.*, 2018, **57**, 5408.
- K. T. Mahmudov, M. N. Kopylovich, M. F. C. Guedes da Silva, A. J. L. Pombeiro, *Dalton Trans.* 2017, **46**, 10121.
- M. Juanes, W. Li, L. Spada, L. Evangelisti, A. Lesarri, W. Caminati, *Phys. Chem. Chem. Phys.* 2019, **21**, 3676.
- M. Juanes, I. Usabiaga, I. Leon, L. Evangelisti, J. A. Fernandez, A. Lesarri, *Angew. Chem. Int. Ed.* 2020, **59**, 14081.
- a)S. T. Shipman, B. H. Pate, in *Handbook of High-Resolution Spectroscopy*, Wiley, New York, 2011; b) J. L. Neill, S. T.

- Shipman, L. Alvarez-Valtierra, A. Lesarri, Z. Kisiel, B. H. Pate, *J. Mol. Spectrosc.* 2011, **269**, 21.
- 30 T. A. Halgren, *J. Comput. Chem.* 1996, **17**, 520.
- 31 MacroModel, Schrödinger Release 2020-1; Schrödinger, LLC: New York, NY, 2020.
- 32 A. D. Becke, *J. Chem. Phys.* 1993, **98**, 5648.
- 33 S. Grimme, J. Antony, S. Ehrlich, H. Krieg, *J. Chem. Phys.* 2010, **132**, 154104.
- 34 a) S. Grimme, S. Ehrlich, L. Goerigk, *J. Comput. Chem.* 2011, **32**, 1456; b) E. R. Johnson, A. D. Becke, *J. Chem. Phys.* 2006, **124**, 174104.
- 35 S. F. Boys, F. Bernardi, *Mol. Phys.* 1970, **19**, 553.
- 36 E. D. Glendening, C. R. Landis, F. Weinhold, *WIREs Comput. Mol. Sci.* 2012, **2**, 1.
- 37 M. J. Frisch, G. W. Trucks, H. B. Schlegel, G. E. Scuseria, M. A. Robb, J. R. Cheeseman, G. Scalmani, V. Barone, B. Mennucci, G. A. Petersson, H. Nakatsuji, M. Caricato, X. Li, H. P. Hratchian, A. F. Izmaylov, J. Bloino, G. Zheng, J. L. Sonnenberg, M. Hada, M. Ehara, K. Toyota, R. Fukuda, J. Hasegawa, M. Ishida, T. Nakajima, Y. Honda, O. Kitao, H. Nakai, T. Vreven, J. A. Montgomery, Jr., J. E. Peralta, F. Ogliaro, M. Bearpark, J. J. Heyd, E. Brothers, K. N. Kudin, V. N. Staroverov, R. Kobayashi, J. Normand, K. Raghavachari, A. Rendell, J. C. Burant, S. S. Iyengar, J. Tomasi, M. Cossi, N. Rega, J. M. Millam, M. Klene, J. E. Knox, J. B. Cross, V. Bakken, C. Adamo, J. Jaramillo, R. Gomperts, R. E. Stratmann, O. Yazyev, A. J. Austin, R. Cammi, C. Pomelli, J. W. Ochterski, R. L. Martin, K. Morokuma, V. G. Zakrzewski, G. A. Voth, P. Salvador, J. J. Dannenberg, S. Dapprich, A. D. Daniels, Ö. Farkas, J. B. Foresman, J. V. Ortiz, J. Cioslowski, D. J. Fox, *Gaussian16*, Revision A.03, Gaussian, Inc., Wallingford, CT, 2016.
- 38 T. Lu, F. Chen, *J. Comput. Chem.* 2012, **33**, 580.
- 39 W. Humphrey, A. Dalke, K. Schulten, *J. Mol. Graphics* 1996, **14**, 33.
- 40 E. R. Johnson, S. Keinan, P. Mori-Sánchez, J. Contreras-García, A. J. Cohen, W. Yang, *J. Am. Chem. Soc.* 2010, **132**, 6498.
- 41 B. Jeziorski, R. Moszynski, K. Szalewicz, *Chem. Rev.* 1994, **94**, 1887.
- 42 R. M. Parrish, L. A. Burns, D. G. A. Smith, A. C. Simmonett, A. E. DePrince, 3rd, E. G. Hohenstein, U. Bozkaya, A. Y. Sokolov, R. Di Remigio, R. M. Richard, J. F. Gonthier, A. M. James, H. R. McAlexander, A. Kumar, M. Saitow, X. Wang, B. P. Pritchard, P. Verma, H. F. Schaefer, 3rd, K. Patkowski, R. A. King, E. F. Valeev, F. A. Evangelista, J. M. Turney, T. D. Crawford, C. D. Sherrill, *J. Chem. Theory Comput.* 2017, **13**, 3185.
- 43 J. K. G. Watson, in *Vibrational Spectra and Structure*, Vol. 6, J. R. Durig, ed., Elsevier, New York/Amsterdam, 1977; Vol. 6, pp. 1-89.
- 44 H. M. Pickett, *J. Mol. Spectrosc.* 1991, **148**, 371-377.
- 45 J.-U. Grabow, in *Handbook of High-Resolution Spectroscopy*, Wiley, New York, 2011.
- 46 R. S. Ruoff, T. D. Klots, T. Emilsson, H. S. Gutowsky, *J. Chem. Phys.* 1990, **93**, 3142.
- 47 W. Caminati, J. C. Lopez, S. Blanco, S. Mata, J. L. Alonso, *Phys. Chem. Chem. Phys.* 2010, **12**, 10230.
- 48 Z. Kisiel, *J. Mol. Spectrosc.* 2003, **218**, 58.
- 49 Y. Jin, X. Li, Q. Gou, G. Feng, J.-U. Grabow, W. Caminati, *Phys. Chem. Chem. Phys.* 2019, **21**, 15656.
- 50 a) T. Lu, Y. Zheng, Q. Gou, G.-L. Hou, G. Feng, *Phys. Chem. Chem. Phys.* 2019, **21**, 24659; b) Y. Jin, T. Lu, G. Feng, *Phys. Chem. Chem. Phys.* 2020, **22**, 28339; c) X. Li, K. G. Lengsfeld, P. Buschmann, J. Wang, J.-U. Grabow, Q. Gou, G. Feng, *J. Mol. Spectrosc.* 2021, **376**, 111409.
- 51 A. E. Reed, R. B. Weinstock, F. Weinhold, *J. Chem. Phys.* 1985, **83**, 735.

View Article Online

DOI: 10.1039/C1CP00079D